



## EFFECTS OF BOUNDARY CONDITIONS ON THE NATURAL FREQUENCIES AND CRITICAL SPEEDS OF ROTATING CYLINDRICAL SHELLS

T. Y. NG<sup>a</sup> and R. E. S. KOH

*School of Mechanical and Aerospace Engineering,  
Nanyang Technological University,  
50 Nanyang Avenue, Singapore 639798. <sup>a</sup>mtyn@ntu.edu.sg*

Accepted 4 September 2011

In this paper, we examine the effects of boundary conditions on the vibration and critical speeds of rotating cylindrical shells. The present work is based on the Love hypothesis for classical thin shells. In addition, the effects due to the shell rotation, namely the centrifugal forces, Coriolis acceleration and initial hoop tension, have been incorporated into the formulation. A Galerkin formulation is presented, with characteristic beam functions being employed to describe the displacement field. Through this numerical procedure, the roots of the determinant of the characteristic matrix of the rotating shell system are calculated, and the natural frequencies and critical speeds can be subsequently obtained. The effects of boundary conditions on the natural frequencies of various modes of vibration of the rotating shells are first examined. Then we investigate the effects of length, axial mode number and boundary conditions, on the critical speeds of the rotating shells.

*Keywords:* Rotating Cylindrical Shell; Vibration and critical speed; Boundary conditions; Galerkin method; Centrifugal forces; Initial hoop tension; Coriolis acceleration.

### 1. Introduction

Over the years, rotating cylindrical shell structures have found significant application areas, such as in turbine power plants, rocketry and missile technology, and rotating cylindrical/drum dryers in chemical processing. The first published work on a rotating shell was carried out by Bryan [1890], where the dynamics of a rotating thin ring were investigated. It was in this study that the travelling-mode phenomenon was discovered. DiTaranto and Lessen [1964] later took into account the effects of Coriolis forces in their study of an infinitely long rotating thin-walled isotropic cylindrical shell, and concluded that Coriolis forces have a significant impact on the natural frequencies of the shell. Subsequently, Srinivasan and Lauterbach [1971] combined both the Coriolis forces and travelling modes phenomena in their study of infinitely long, rotating isotropic cylindrical shells. For a non-rotating cylindrical shell, its vibration is in the form of a standing wave motion.

With rotation, the presence of Coriolis and centrifugal forces, creates a bifurcation phenomenon leading to the emergence of backward and forward waves.

It is due to the existence of forward waves that at a certain critical rotating speed, the cylindrical shell may become dynamically unstable, even in the absence of a compressive load. This instability phenomenon occurs only for certain modes, and early works which studied the critical speed phenomenon include those of Brzoska [1953] and Grybos [1961], where Love's first approximation was used to obtain the critical speeds for a special case of a thin-walled cylinder. Experimentally, critical speed results for rotating shells have been obtained and reported by Zinberg and Symonds [1970]. However, there seems to be limited works which report the effects of different boundary conditions on the critical speeds of rotating cylindrical shells. Most of the earlier works were focused on the effects of boundary conditions on the natural frequencies, such as those of Koval and Cranch [1962], Chung [1981] and Lam and Loy [1998].

In the present work, we study the effects of boundary conditions on the vibration and the critical speeds of rotating cylindrical shells under static axial loading. The present work is based on the Love hypothesis for classical thin shells, with consideration of the centrifugal forces, Coriolis acceleration and initial hoop tension. A numerical Galerkin formulation with characteristic beam functions as basis is then formulated to obtain the natural frequencies and critical speeds of the rotating shells. In addition to the effects of boundary conditions, the effects of length and axial mode number on the critical speed values of the rotating shells, are also investigated.

## 2. Theory and Formulation

The mathematical theory governing the vibration of thin rotating cylindrical shells is carried out using Love's shell theory, and takes into account the effects of Coriolis, centrifugal forces and the initial hoop tension. Figure 1 shows the nomenclature of a thin, uniform shell of length  $L$ , thickness  $h$ , and radius  $R$ , rotating at constant speed  $\Omega$  about its longitudinal axis. The reference surface of the orthogonal coordinate system is taken to be at the centre of the shell's surface. The longitudinal, circumferential, and radial directions are respectively denoted by  $x$ ,  $\theta$  and  $z$ , and the displacement field of the shell in the respective directions are denoted by  $u$ ,  $v$ , and  $w$ . For a thin shell under plane stress condition, the two-dimensional Hooke's law relation is given by

$$\{\sigma\} = [Q] \{\varepsilon\} \quad (1)$$

where  $\{\sigma\}$  and  $\{\varepsilon\}$  are the stress and strain vectors, respectively, and  $[Q]$  is the stiffness matrix. The stress vector  $\{\sigma\}$  is given by

$$\{\sigma\}^T = \{\sigma_x \quad \sigma_\theta \quad \sigma_{x\theta}\} \quad (2)$$

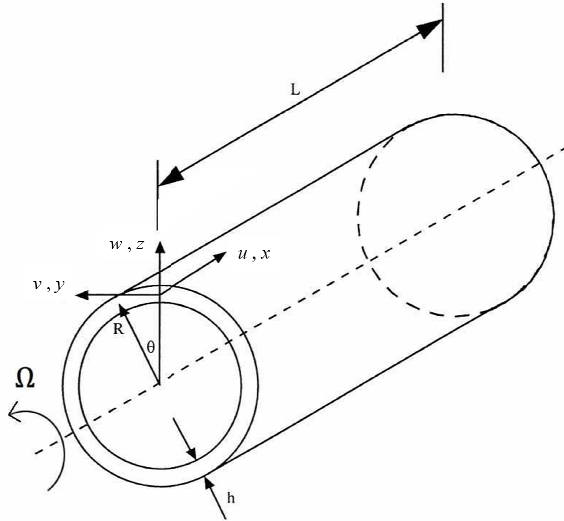


Fig. 1. Nomenclature of the rotating thin cylindrical shell.

where  $\sigma_x$  and  $\sigma_\theta$  are the stresses in the  $x$  and  $\theta$  directions respectively, and  $\sigma_{x\theta}$  is the shear stress in the  $x\theta$  plane. The strain vector  $\{\varepsilon\}$  is

$$\{\varepsilon\}^T = \{\varepsilon_x \ \varepsilon_\theta \ \varepsilon_{x\theta}\} \tag{3}$$

where  $\varepsilon_x$  and  $\varepsilon_\theta$  are the strain components in the  $x$  and  $\theta$  directions respectively, and  $\varepsilon_{x\theta}$  is the shear strain component on the  $x\theta$  plane.

The Love-type shell theory defines the strain components as linear functions of the thickness coordinate  $z$  [5], as follow

$$\begin{aligned} \varepsilon_x &= e_x + zk_1 \\ \varepsilon_\theta &= e_\theta + zk_2 \\ \varepsilon_{x\theta} &= e_{x\theta} + z\tau \end{aligned} \tag{4}$$

where  $e_x$ ,  $e_\theta$  and  $e_{x\theta}$  are the reference strains, and  $k_1$ ,  $k_2$  and  $\tau$  are the reference surface curvatures. They are defined according to Love's shell theory as follow

$$\begin{aligned} \{e_x, e_\theta, e_{x\theta}\} &= \left\{ \frac{\partial u}{\partial x}, \frac{1}{R} \left( \frac{\partial v}{\partial \theta} + w \right), \frac{\partial v}{\partial x} + \frac{1}{R} \frac{\partial u}{\partial \theta} \right\} \\ \{k_1, k_2, \tau\} &= \left\{ -\frac{\partial^2 w}{\partial x^2}, \frac{1}{R^2} \left( -\frac{\partial^2 w}{\partial \theta^2} + \frac{\partial v}{\partial \theta} \right), \frac{2}{R} \left( -\frac{\partial^2 w}{\partial x \partial \theta} + \frac{\partial v}{\partial x} \right) \right\} \end{aligned} \tag{5}$$

Substituting Eq. (5) into Eq. (4), the strain vector is obtained

$$\begin{Bmatrix} \varepsilon_x \\ \varepsilon_\theta \\ \varepsilon_{x\theta} \end{Bmatrix} = \begin{Bmatrix} \frac{\partial u}{\partial x} \\ \frac{1}{R} \left( \frac{\partial v}{\partial \theta} + w \right) \\ \frac{\partial v}{\partial x} + \frac{1}{R} \frac{\partial u}{\partial \theta} \end{Bmatrix} + z \begin{Bmatrix} -\frac{\partial^2 w}{\partial x^2} \\ \frac{1}{R^2} \left( -\frac{\partial^2 w}{\partial \theta^2} + \frac{\partial v}{\partial \theta} \right) \\ \frac{2}{R} \left( -\frac{\partial^2 w}{\partial x \partial \theta} + \frac{\partial v}{\partial x} \right) \end{Bmatrix} \tag{6}$$

For an isotropic shell, the stiffness matrix is given as

$$[Q] = \begin{bmatrix} Q_{11} & Q_{12} & 0 \\ Q_{12} & Q_{22} & 0 \\ 0 & 0 & Q_{66} \end{bmatrix} \tag{7}$$

where the elements  $Q_{ij}$  are defined as

$$Q_{11} = Q_{22} = \frac{E}{1 - \mu^2}, Q_{12} = \frac{E\mu}{1 - \mu^2}, Q_{66} = G \tag{8}$$

and  $E$  and  $G$  and  $\mu$  are the Young modulus, shear modulus and Poisson's ratio of the shell's material, respectively.

Substituting Eqs. (4) and (7) into Eq. (1), the following is obtained

$$\{\sigma\} = \begin{bmatrix} Q_{11} & Q_{12} & 0 & zQ_{11} & zQ_{12} & 0 \\ Q_{12} & Q_{22} & 0 & zQ_{12} & zQ_{22} & 0 \\ 0 & 0 & Q_{66} & 0 & 0 & zQ_{66} \end{bmatrix} \{e\} \tag{9}$$

where  $\{e\}$  is the component strain vector which can be written as

$$\{e\}^T = \{e_x, e_\theta, e_{x\theta}, k_1, k_2, \tau\} \tag{10}$$

The force and moment resultants can thus be defined as

$$\{N_x, N_\theta, N_{x\theta}\} = \int_{-h/2}^{h/2} \{\sigma_x, \sigma_\theta, \sigma_{x\theta}\} dz \tag{11}$$

$$\{M_x, M_\theta, M_{x\theta}\} = \int_{-h/2}^{h/2} \{\sigma_x, \sigma_\theta, \sigma_{x\theta}\} z dz \tag{12}$$

Substituting the stress vector in Eq. (9) into the force and moment resultants in Eqs. (11) and (12) yields the constitutive equation for a cylindrical shell

$$\{N\} = [S] \{e\} \tag{13}$$

where  $\{N\}$  is the combination vector of the force and moment resultants from Eqs. (11) and (12)

$$\{N\}^T = \{N_x, N_\theta, N_{x\theta}, M_x, M_\theta, M_{x\theta}\} \tag{14}$$

and  $[S]$  is the stiffness matrix

$$[S] = \begin{pmatrix} A & B \\ B & D \end{pmatrix} \tag{15}$$

where  $A$ ,  $B$  and  $D$  are  $3 \times 3$  matrices of the extensional stiffness, coupling stiffness and bending stiffness of the cylindrical shell, respectively. For a thin cylindrical shell, they are defined as

$$A_{ij} = \int_{-h/2}^{h/2} Q_{ij} dz, B_{ij} = \int_{-h/2}^{h/2} Q_{ij} z dz, D_{ij} = \int_{-h/2}^{h/2} Q_{ij} z^2 dz \tag{16}$$

where  $Q_{ij}$  ( $i, j=1, 2, 6$ ) are elements of the shell's stiffness matrix defined in Eq. (8).

For an isotropic cylindrical shell, the force and moment resultants are obtained as follows

$$N_x = \frac{Eh}{1-\mu^2} (e_x + \mu e_\theta) = \frac{Eh}{1-\mu^2} \left[ \frac{\partial u}{\partial x} + \frac{\mu}{R} \left( \frac{\partial v}{\partial \theta} + w \right) \right] \quad (17)$$

$$N_\theta = \frac{Eh}{1-\mu^2} (\mu e_x + e_\theta) = \frac{Eh}{1-\mu^2} \left[ \mu \frac{\partial u}{\partial x} + \frac{1}{R} \left( \frac{\partial v}{\partial \theta} + w \right) \right] \quad (18)$$

$$N_{x\theta} = \frac{Eh}{2(1+\mu)} (e_{x\theta}) = \frac{Eh}{2(1+\mu)} \left[ \frac{\partial v}{\partial x} + \frac{1}{R} \frac{\partial u}{\partial \theta} \right] \quad (19)$$

$$M_x = \frac{Eh^3}{12(1-\mu^2)} (k_1 + \mu k_2) = \frac{Eh^3}{12(1-\mu^2)} \left[ -\frac{\partial^2 w}{\partial x^2} + \frac{\mu}{R^2} \left( -\frac{\partial^2 w}{\partial \theta^2} + \frac{\partial v}{\partial \theta} \right) \right] \quad (20)$$

$$M_\theta = \frac{Eh^3}{12(1-\mu^2)} (\mu k_1 + k_2) = \frac{Eh^3}{12(1-\mu^2)} \left[ -\mu \frac{\partial^2 w}{\partial x^2} + \frac{1}{R^2} \left( -\frac{\partial^2 w}{\partial \theta^2} + \frac{\partial v}{\partial \theta} \right) \right] \quad (21)$$

$$M_{x\theta} = \frac{Eh^3}{24(1+\mu)} (\tau) = \frac{Eh^3}{12(1+\mu)} \left[ \frac{1}{R} \left( -\frac{\partial^2 w}{\partial x \partial \theta} + \frac{\partial v}{\partial x} \right) \right] \quad (22)$$

The equations of motion for a rotating cylindrical shell, as given by Srinivasan and Lauterbach [1971] are

$$L_x(u, v, w) - \rho h \frac{\partial^2 u}{\partial t^2} = 0 \quad (23)$$

$$L_\theta(u, v, w) - \rho h \left( \frac{\partial^2 v}{\partial t^2} + 2\Omega \frac{\partial w}{\partial t} - \Omega^2 v \right) = 0 \quad (24)$$

$$L_z(u, v, w) - \rho h \left( \frac{\partial^2 w}{\partial t^2} + 2\Omega \frac{\partial v}{\partial t} - \Omega^2 w \right) = 0 \quad (25)$$

where  $\rho$  is the density of the shell. In addition, the two terms  $\Omega^2 v$  and  $\Omega^2 w$  in Eqs. (24) and (25) are the centrifugal terms, while the two terms  $2\Omega \frac{\partial w}{\partial t}$  and  $2\Omega \frac{\partial v}{\partial t}$  are the Coriolis terms. The differential operators  $L_x(u, v, w)$ ,  $L_\theta(u, v, w)$  and  $L_z(u, v, w)$  are defined according to Love's shell theory as

$$L_x = \frac{\partial N_x}{\partial x} + \frac{1}{R} \frac{\partial N_{x\theta}}{\partial \theta} + \tilde{N}_\theta \left( \frac{1}{R^2} \frac{\partial^2 u}{\partial \theta^2} - \frac{1}{R} \frac{\partial w}{\partial x} \right) \quad (26)$$

$$L_\theta = \frac{\partial N_{x\theta}}{\partial x} + \frac{1}{R} \frac{\partial N_\theta}{\partial \theta} + \frac{1}{R} \frac{\partial M_{x\theta}}{\partial x} + \frac{1}{R^2} \frac{\partial M_\theta}{\partial \theta} + \frac{\tilde{N}_\theta}{R} \frac{\partial^2 u}{\partial x \partial \theta} \quad (27)$$

$$L_z = \frac{\partial^2 M_x}{\partial x^2} + \frac{2}{R} \frac{\partial^2 M_{x\theta}}{\partial x \partial \theta} + \frac{1}{R^2} \frac{\partial^2 M_\theta}{\partial \theta^2} - \frac{N_\theta}{R} + \frac{\tilde{N}_\theta}{R} \left( \frac{\partial^2 w}{\partial \theta^2} - \frac{\partial v}{\partial \theta} \right) \quad (28)$$

where  $N_x$ ,  $N_\theta$ ,  $N_{x\theta}$ ,  $M_x$ ,  $M_\theta$ ,  $M_{x\theta}$  are the force and moment resultants defined in Eqs. (17) to (22), and  $\tilde{N}_\theta$  is the initial hoop tension due to the centrifugal force,

and is defined as

$$\tilde{N}_\theta = \rho h \Omega^2 R^2 \tag{29}$$

After performing the relevant substitutions the equations of motion, Eqs. (23) to (25), can be written as

$$R^2 \frac{\partial^2 u}{\partial x^2} + \mu R \frac{\partial w}{\partial x} + \frac{1}{2} (1 - \mu) \frac{\partial^2 u}{\partial \theta^2} + \frac{R}{2} (1 + \mu) \frac{\partial^2 v}{\partial x \partial \theta} + \frac{\gamma}{\rho h} \tilde{N}_\theta \left( \frac{1}{R^2} \frac{\partial^2 u}{\partial \theta^2} - \frac{1}{R} \frac{\partial w}{\partial x} \right) = \gamma \frac{\partial^2 u}{\partial t^2} \tag{30}$$

$$\begin{aligned} & \frac{R^2}{2} (1 - \mu) \frac{\partial^2 v}{\partial x^2} + \frac{R}{2} (1 + \mu) \frac{\partial^2 u}{\partial x \partial \theta} + \frac{\partial^2 v}{\partial \theta^2} + \frac{\partial w}{\partial \theta} \\ & + k \left[ R^2 (1 - \mu) \frac{\partial^2 v}{\partial x^2} - R^2 \frac{\partial^3 w}{\partial x^2 \partial \theta} - \frac{\partial^3 w}{\partial \theta^3} + \frac{\partial^2 v}{\partial \theta^2} \right] \\ & + \frac{\gamma}{\rho h} \frac{\tilde{N}_\theta}{R} \frac{\partial^2 u}{\partial x \partial \theta} = \gamma \left( \frac{\partial^2 v}{\partial t^2} + 2\Omega \frac{\partial w}{\partial t} - \Omega^2 v \right) \end{aligned} \tag{31}$$

$$\begin{aligned} & -\mu R \frac{\partial u}{\partial x} - \frac{\partial v}{\partial \theta} - w - k \left( R^4 \frac{\partial^4 w}{\partial x^4} + \frac{\partial^4 w}{\partial \theta^4} + 2R^2 \frac{\partial^4 w}{\partial x^2 \partial \theta^2} \right) \\ & + k \left[ \frac{\partial^3 v}{\partial \theta^3} + R^2 (2 - \mu) \frac{\partial^3 v}{\partial x^2 \partial \theta} \right] \\ & + \frac{\gamma}{\rho h} \frac{\tilde{N}_\theta}{R^2} \left( \frac{\partial^2 w}{\partial \theta^2} - \frac{\partial v}{\partial \theta} \right) = \gamma \left( \frac{\partial^2 w}{\partial t^2} + 2\Omega \frac{\partial v}{\partial t} - \Omega^2 w \right) \end{aligned} \tag{32}$$

where  $\gamma = \frac{\rho R^2 (1 - \mu^2)}{E}$  and  $k = \frac{h^2}{12R^2}$ .

The solutions to the three partial differential equations, Eqs. (30) to (32), for a rotating cylindrical shell can be expressed as follow

$$\begin{aligned} u(x, \theta, t) &= A \varphi_u(x) \phi_u(\theta, t) \\ v(x, \theta, t) &= B \varphi_v(x) \phi_v(\theta, t) \\ w(x, \theta, t) &= C \varphi_w(x) \phi_w(\theta, t) \end{aligned} \tag{33}$$

where  $A$ ,  $B$  and  $C$  are constants representing the displacement amplitudes of the vibration in the respective axes. The circumferential modal function  $\phi_i(\theta, t)$  ( $i = u, v, w$ ) can be written as

$$\begin{aligned} \phi_u(\theta, t) &= \phi_w(\theta, t) = \cos(n\theta + \omega t) \\ \phi_v(\theta, t) &= \sin(n\theta + \omega t) \end{aligned} \tag{34}$$

where  $n$  is an integer representing the circumferential wave number. The function  $\varphi_i(x)$  ( $i = v, w$ ) represents the respective axial mode shapes and the characteristic

beam functions with the required boundary conditions can be assumed here.  $\varphi_u(x)$  is taken as the partial derivative of  $\varphi_i(x)$  ( $i = v, w$ ) with respect to  $x$ , i.e.

$$\varphi_u(x) = \frac{\partial \varphi_i(x)}{\partial x}, (i = v, w) \tag{35}$$

The axial modal functions need to satisfy the boundary conditions applied at the two open ends of the shell, i.e. at  $x=0$  and  $x=L$ . These can be expressed as

$$\varphi(x) = \frac{\partial^2 \varphi(x)}{\partial x^2} = 0 \text{ (Simply-Supported)}$$

$$\varphi(x) = \frac{\partial \varphi(x)}{\partial x} = 0 \text{ (Clamped)}$$

$$\varphi \frac{\partial^2 \varphi(x)}{\partial x^2} = \frac{\partial \varphi^3(x)}{\partial x^3} = 0 \text{ (Free)}$$

The beam functions  $\varphi(x)$  for the different boundary conditions cases studied in this work are thus given as follow:

*Simply-Supported — Simply-Supported (SS-SS)*

$$\varphi(x) = \sin\left(\frac{m\pi x}{L}\right) \tag{36}$$

where  $m = 1, 2, 3 \dots$

*Clamped-Clamped (C-C)*

$$\varphi(x) = \cosh\left(\frac{\lambda_m x}{L}\right) - \cos\left(\frac{\lambda_m x}{L}\right) - \frac{\cosh(\lambda_m) - \cos(\lambda_m)}{\sinh(\lambda_m) - \sin(\lambda_m)} \left[ \sinh\left(\frac{\lambda_m x}{L}\right) - \sin\left(\frac{\lambda_m x}{L}\right) \right] \tag{37}$$

where  $\cos \lambda_m \cosh \lambda_m = 1$

*Simply-Supported-Clamped (SS-C)*

$$\varphi(x) = \sinh\left(\frac{\lambda_m x}{L}\right) - \frac{\sinh(\lambda_m)}{\sin(\lambda_m)} \sin\left(\frac{\lambda_m x}{L}\right) \tag{38}$$

where  $\tan \lambda_m = \tanh \lambda_m$

*Free-Free (FF)*

$$\varphi(x) = \cosh\left(\frac{\lambda_m x}{L}\right) + \cos\left(\frac{\lambda_m x}{L}\right) - \frac{\cosh(\lambda_m) - \cos(\lambda_m)}{\sinh(\lambda_m) - \sin(\lambda_m)} \left[ \sinh\left(\frac{\lambda_m x}{L}\right) + \sin\left(\frac{\lambda_m x}{L}\right) \right] \tag{39}$$

where  $\cos \lambda_m \cosh \lambda_m = 1$

To solve for the natural frequencies of the rotating shell with the different boundary conditions, Eqs. (30) to (32) are rewritten respectively as

$$L_{11}u + L_{12}v + L_{13}w = 0 \tag{40}$$

$$L_{21}u + L_{22}v + L_{23}w = 0 \tag{41}$$

$$L_{31}u + L_{32}v + L_{33}w = 0 \tag{42}$$

where  $L_{ij}(i, j = 1, 2, 3)$  are the differential operators of  $u, v$ , and  $w$ . Substituting

the modal functions into the governing equations and applying Galerkin's method gives

$$\int_0^{\frac{2\pi}{\omega}} \int_0^{2\pi} \int_0^L (L_{ij}u + L_{ij}v + L_{ij}w) \varphi_k \, dx \, d\theta \, dt = 0 \tag{43}$$

for the indices  $(i,j=1,2,3)$  and  $(k=u,v,w)$ . The three resulting equations can then be written in matrix form as

$$\begin{bmatrix} C_{11} & C_{12} & C_{13} \\ C_{21} & C_{22} & C_{23} \\ C_{31} & C_{32} & C_{33} \end{bmatrix} \begin{Bmatrix} A \\ B \\ C \end{Bmatrix} = \begin{Bmatrix} 0 \\ 0 \\ 0 \end{Bmatrix} \tag{44}$$

Finally, to solve for non-trivial solutions in the above equation, the determinant of the characteristic matrix  $[C_{ij}]$  is set to zero, and the unknown frequencies  $\omega$  can be solved numerically by any appropriate root solver.

### 3. Results and Discussions

The frequency results in this work are all normalized against the natural frequency of a non-rotating cylindrical shell of SS-SS boundary condition, and corresponding to the mode  $m = 1$  and  $n = 1$ . Additional parameters of the shell used for normalization are  $L/R = 6$  and  $h/R = 1$ .

First we shall examine how the natural frequencies vary with the shell rotating speed for the four boundary condition cases considered here. The calculated results are shown in Fig. 2 for mode  $m = 1$  and various cases of circumferential wave numbers,  $n$ , are investigated. We note the order of the different boundary condition

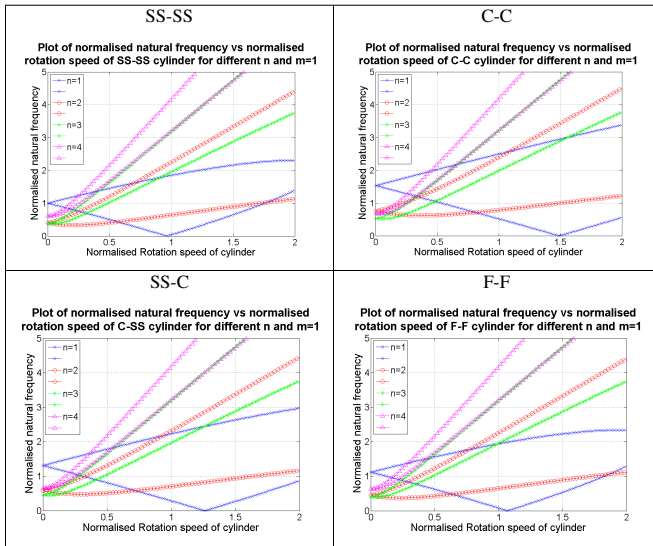


Fig. 2. Variation of the normalized natural frequency with rotating speed for thin isotropic shells of different boundary conditions ( $m = 1$ ,  $L/R = 6$  and  $h/R = 0.02$ ).



cases with respect to increasing natural frequencies, which follow generally follow the order of SS-SS→F-F→SS-C→C-C. The results also illustrate that at zero rotation speed, there is a trend of decreasing natural frequencies as  $n$  increases from 1 to 3, after which they begin to increase for  $n > 3$ . As  $n$  increases further, one also observed the convergence of the natural frequencies to common values for all the four boundary conditions cases. Figure 2 also shows that for all four boundary condition cases, critical rotating speed only occurs for modes where  $n = 1$ , and with rotation, the natural frequencies decrease for all boundary condition cases at this mode, and the frequencies eventually approach zero when their critical rotating speeds are reached. For modes where  $n \geq 3$ , the natural frequencies generally increase with rotation speed.

Next we examine variation of the natural frequencies with  $m$  and  $n$  for the different boundary condition cases. The results are shown in Fig. 3, where two plots are generated for each of the boundary conditions, namely for a non-rotating shell and one which rotates at 100 rev/s. The rotation speed of 100 rev/s is chosen because it is the speed which is close to the critical rotating speed of the cylindrical

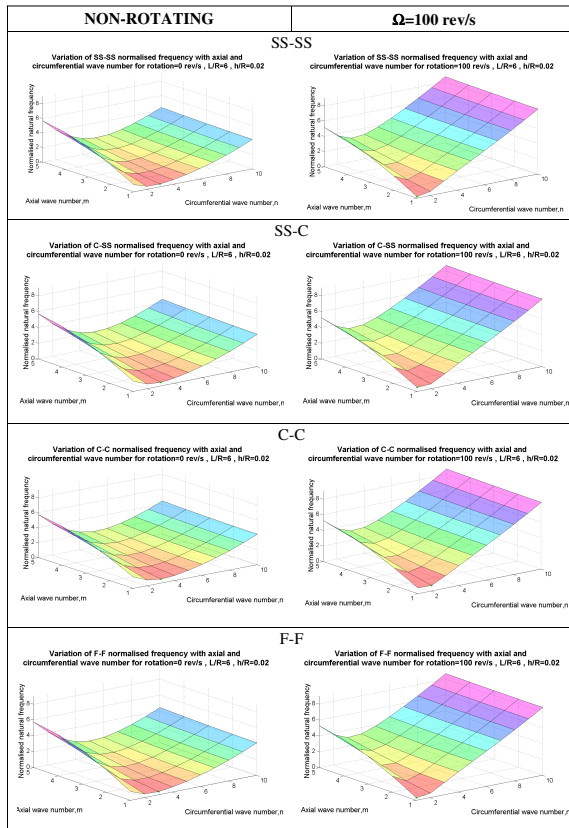


Fig. 3. Variation of normalized natural frequencies with modal parameters  $m$  and  $n$  for a thin isotropic shell ( $L/R = 6$  and  $h/R = 0.02$ ).

shells considered here. In addition, the minimum frequency is indicated on the plots as a green dot. From Fig. 3, we observe that the most significant effect of rotation is the decrease of the natural frequencies for the modes associated with  $n = 1$  and  $2$ , and an increase in natural frequencies for modes where  $n > 3$ . The fundamental frequency also changes from mode  $(m = 1, n = 3)$  to mode  $(m = 1, n = 1)$  with the increase in rotation speed, for all four boundary condition cases. This is to be expected as there exists a critical rotating speed for modes involving  $n = 1$ , where the fundamental frequency decreases to zero with increasing rotation speed. For all four boundary conditions, we can see that at all values of  $n$ , the vibration frequency increases as  $m$  increases. However, these increases are much greater at low values of  $n$ , and this applies for both for non-rotating and rotating cases. Therefore, at high  $n$  values, the change in  $m$  has less effect on the natural frequencies.

We now move on to study the influence of shell thickness on the natural frequencies of the rotating shells. Figure 4 shows the results for two different thicknesses for

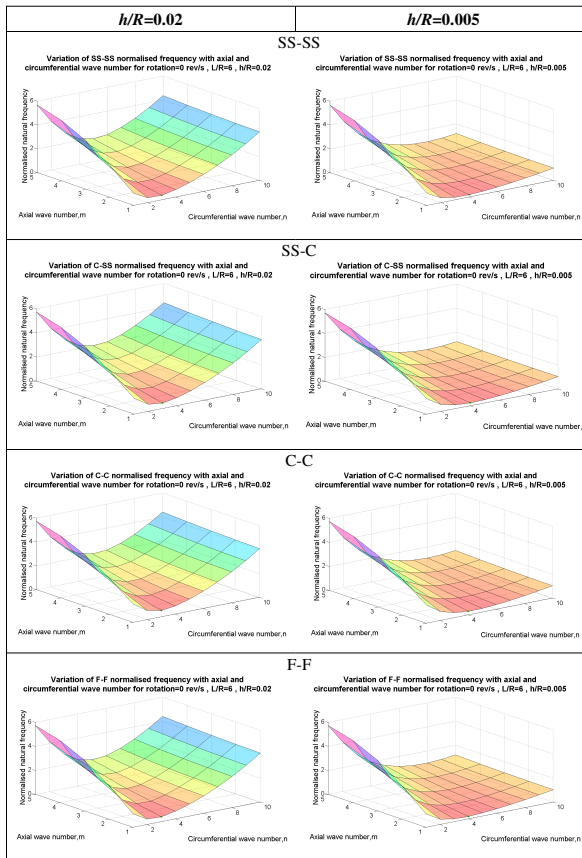


Fig. 4. Variation of normalized natural frequencies with modal parameters  $m$  and  $n$  for a non-rotating thin isotropic shell ( $L/R = 6$ ).

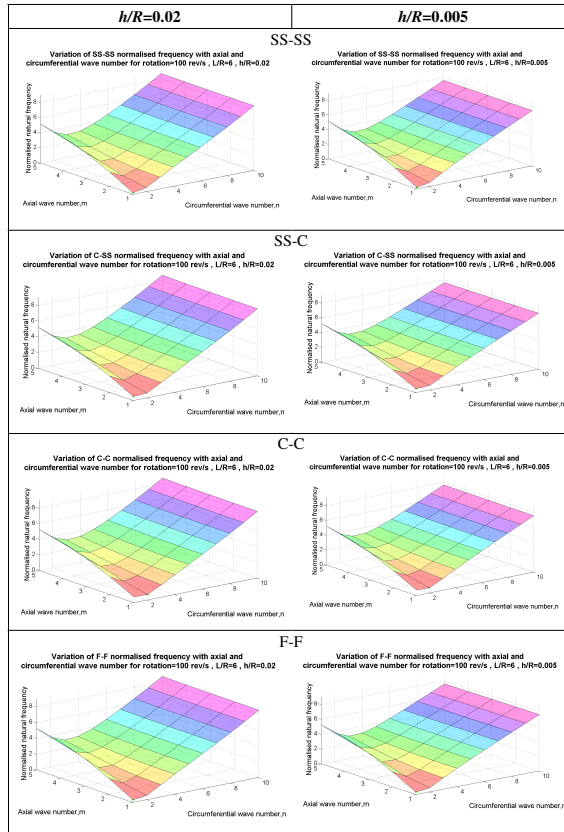


Fig. 5. Variation of normalized natural frequencies with modal parameters  $m$  and  $n$  for a thin isotropic shell rotating at 100rev/s ( $L/R = 6$ ).

a non-rotating shell, namely  $h/R = 0.02$  and  $h/R = 0.005$ , while Fig. 5 shows the corresponding results for a shell rotating at 100 rev/s. Examining the non-rotating case first in Fig. 4, the plots show that the change in thickness only has significant effects on the natural frequencies for the modes involving  $n > 3$ . At these  $n$  values, a thinner shell thickness results in lower natural frequencies for all  $m$  values. At the original  $h/R$  ratio of 0.02, the  $n$  value associated with the fundamental frequency is 3. However, a qualitative change occurs when the  $h/R$  ratio is reduced to 0.005, when we observe that the fundamental frequency is now associated with  $n = 4$ . For the rotating cases in Fig. 5, we observe a similar trend as the non-rotating cases in that the change in thickness only affects the natural frequencies for modes involving  $n > 3$ . With decreasing thickness, the natural frequencies drop for all  $m$  values, however, the drop is not as high compared to the corresponding non-rotating cases.

The phenomenon of critical rotating speed only exists for modes involving  $n=1$ . Here we examine how the critical speeds are affected by changes in two parameters, namely the  $L/R$  ratio and  $m$  value. Figure 6 shows how the critical rotating speed

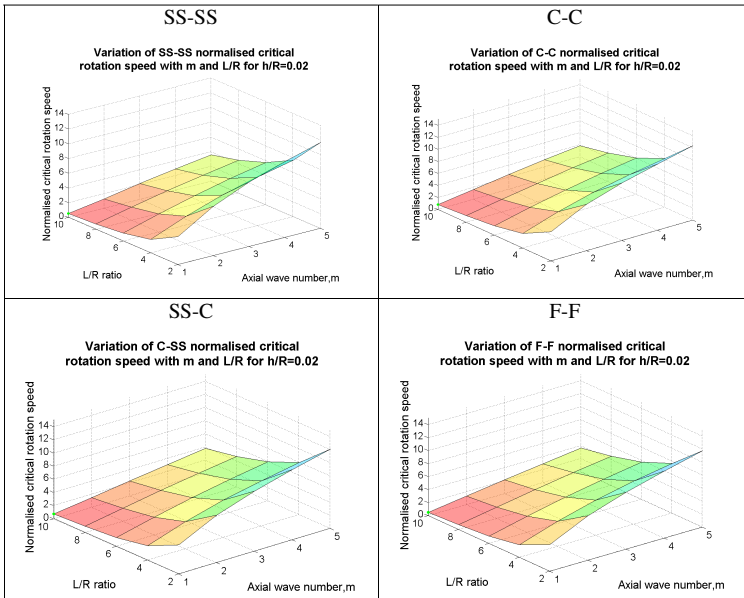


Fig. 6. Variation of normalized critical rotating speed with  $m$  and  $L/R$  for a thin isotropic cylindrical shell ( $n = 1, h/R = 0.02$ ).

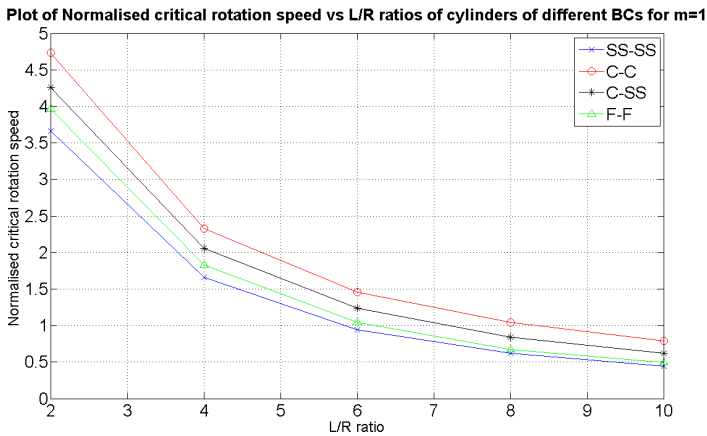


Fig. 7. Variation of normalized critical rotating speed with  $L/R$  ratio for thin isotropic shells of different boundary conditions ( $m = 1, n = 1, h/R = 0.02$ ).

varies with these two parameters, for the four boundary condition cases studied in this work. The trends observed for all four different boundary condition cases are very similar. The figure reveals that longer length cylindrical shells, and lower  $m$  values, lead to lower critical rotating speeds. Figures 7 and 8 respectively show another view of the effects of varying the parameters,  $L/R$  and  $m$ , on the critical

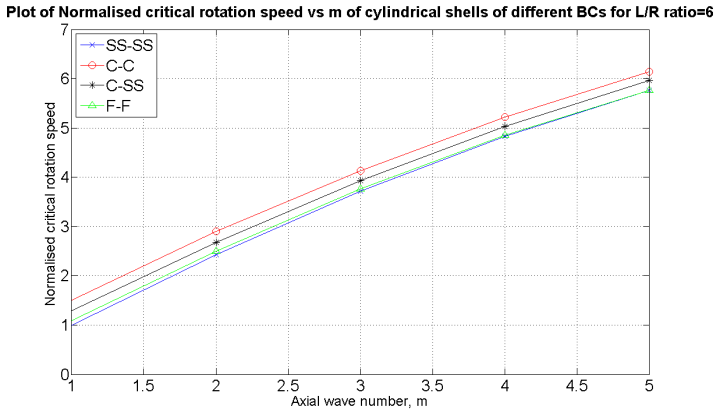


Fig. 8. Variation of normalized critical rotating speed with axial wave number  $m$  for thin isotropic shells of different boundary conditions ( $n = 1$ ,  $h/R = 0.02$ ,  $L/R = 6$ ).

speeds of the rotating shell. It can now be clearly observed that the drop in critical rotating speed for increasing  $L/R$  ratios is nonlinear, and the effect becomes less significant when the ratio reaches about 10. On the other hand, the increase in critical rotating speed with increasing  $m$  value is quite linear.

#### 4. Conclusions

Using Love's theory for thin shells and the numerical implementation of Galerkin's method, the vibration characteristics of rotating thin isotropic cylindrical shells of different boundary conditions were investigated. The parameters whose effects on the natural frequencies and critical speeds were examined include the axial and circumferential wave numbers and the shell thickness. It was found that before critical rotating speeds are reached, cylindrical shells with SS-SS boundary conditions has the lowest natural frequency, followed by F-F, C-SS and C-C cases, in that order. For non-rotating shells with a value of length-to-radius ratio of six, the fundamental frequency occurs at mode ( $m=1$ ,  $n=2$  or  $3$ ) depending on the boundary conditions. However, as the shell becomes a rotating one, a qualitative change occurs, and the mode ( $m=1$ ,  $n=1$ ) becomes the fundamental mode. For the study on critical rotating speeds, it was found that the shorter length shells possess higher critical rotating speeds. Also, higher axial wave numbers are generally associated with higher critical rotating speed.

#### References

- Bryan, G. H. [1890] "On the beats in the vibration of revolving cylinder or bell," *Proceedings of the Cambridge Philosophical Society* **7**, 101–111.  
 Brzoska, Z. A. [1953] "Critical speeds of short drums," *Tech Lotn* **8**, 151–156.

- Chung, H. [1981] "Free vibration analysis of circular cylindrical shells," *Journal of Sound and Vibration* **74**, 331–350.
- DiTaranto, R. A. and Lessen, M. [1964] "Coriolis acceleration effect on the vibration of a rotating thin-walled circular cylinder," *ASME Journal of Applied Mechanics* **31**, 700–701.
- Grybos, R. [1961] *Dialogue Concerning Two New Sciences-1638*, Northwestern University Press, Evanston, Illinois.
- Koval, L. R. and Cranch, E. T. [1962] "On the free vibrations of thin cylindrical shells subjected to an initial torque," *Proceedings of the 4<sup>th</sup> US Congress of Applied Mechanics*, 107–117.
- Lam, K. Y. and Loy, C. T. [1998] "Influence of boundary conditions for a thin laminated rotating cylindrical shell," *Composite Structures* **41**, 215–228.
- Srinivasan, A. V. and Lauterbach, G. F. [1971] "Travelling waves in rotating cylindrical shells," *ASME Journal of Engineering for Industries* **93**, 1229–1232.
- Zinberg, H. and Symonds, M. F. [1970] "The development of advanced composite tail rotor driveshaft," *Proceedings of the 26<sup>th</sup> Annual Forum of the American Helicopter Society*, 1–14.